TOWARDS THE LIMITS OF STABILITY — NEW DECAY STUDY OF THE LIGHTEST MENDELEVIUMS*

S. Kumar [a,b], D. Ackermann [a], J. Piot [a], D. Seweryniak [c]
V. Karayonchev[c], S. Antalic[d], Ch. Stodel[a], A. Bahini[a,†]
B. Andel[d], K. Bhatt[c,e], C. Burns[f], M. Carpenter[c], R. Chakma[c]
A. Ertoprak[c], K. Hauschild[g], F.G. Kondev[c], A. Korichi[c,g]
T. Lauritsen[c], A. Lopez-Martens[g], A. McFarlane[h], J. Mišt[d]
C. Müller-Gatermann[c], D. Potterveld[c], S. Raeder[i]
W. Reviol[c], H. Savajols[a], N. Sensharma[c], R.S. Sidhu[j]
M. Siciliano[c], B. Sulignano[k]

[a]Grand Accélérateur National d'Ions Lourds (GANIL), Caen, France
[b]Université de Caen Normandie, Caen, France
[c]Argonne National Laboratory, Lemont, Illinois, USA
[d]Comenius University in Bratislava, Bratislava, Slovakia
[e]University of Notre Dame, Indiana, USA
[f]University of Massachusetts Lowell, Lowell, Massachusetts, USA
[g]IJCLab, Orsay, France
[h]University of York, York, United Kingdom
[i]GSI Helmholtzzentrum für Schwerionenforschung GmbH, Darmstadt, Germany
[j]University of Surrey, Guildford, United Kingdom
[k]IRFU/DPhN, CEA Saclay, France

Received 8 November 2025, accepted 10 February 2026, published online 31 March 2026

Recent decay studies of ^{244,245}Md at the GSI Helmholtzzentrum für Schwerionenforschung, Germany, and at the Lawrence Berkeley National Laboratory (LBNL) reported conflicting mass assignments to similar α-decay energies. This prompted a new experiment at the Fragment Mass Analyzer (FMA) at Argonne National Laboratory. Using the reaction ^{209}Bi(^{40}Ar, xn)$^{249-x}$Md, we performed simultaneous A/q identification and α-decay energy measurement for neutron-deficient Md isotopes. Correlated recoil-α-decay chains belonging to ^{247}Md and ^{245}Md were identified. Probabilistic mass identification was performed from focal-plane position using a test reaction, yielding consistent $A = 247$ and $A = 245$ mass assignments within uncertainties. This study re-examines the production cross sections, decay energies, and isotopic assignments for the ^{247}Md and ^{245}Md nuclei.

DOI:10.5506/APhysPolBSupp.19.1-A24

* Presented at the XXXVIII Mazurian Lakes Conference on Physics, Piaski, Poland, August 31–September 6, 2025.

† Present address: Université de Caen Normandie, ENSICAEN, CNRS/IN2P3, LPC Caen UMR6534, 14000 Caen, France.

1. Introduction

In the region of heavy actinides, α–γ spectroscopy and isomer studies of odd-A mendelevium (Md, $Z = 101$) and einsteinium (Es, $Z = 99$) isotopes reveal the evolution of low-lying one-quasiparticle states and thus provide access to the changing single-particle shell structure as the neutron number decreases. In particular, the mendelevium isotopes lie immediately above the deformed proton shell gap at $Z = 100$, making these isotopes a sensitive probe of proton Nilsson orbital states near the Fermi surface. The α-decay chains of mendelevium populate isotopes of einsteinium and berkelium (Bk, $Z = 97$), allowing for the study of deformed single-particle orbitals such as $\pi 7/2^-[514]$, $\pi 1/2^-[521]$, $\pi 7/2^+[633]$ and $\pi 3/2^-[521]$ [1].

In the last three decades, fusion–evaporation reactions have been used to study the most neutron-deficient mendelevium isotopes, ^{244,245}Md, using projectiles such as ^{40}Ar and ^{50}Ti on ^{209}Bi and ^{197}Au targets, respectively [2–4]. However, the recent studies of the most neutron-deficient Md isotopes (^{244,245}Md) in 2020, at GSI, TASCA (TransActinide Separator and Chemistry Apparatus) [5] and LBNL, BGS (Berkeley Gas-filled Separator) [6], have shown some inconsistency in the reported results. The α-decay energies reported in both experiments for the mendelevium decay are similar but differ in isotope assignment. While in the experiment at GSI, Khuyagbaatar *et al.* [4] attributed these energies to the decay of ^{245}Md, Pore *et al.* [3] report the same decay energies to belong to ^{244}Md. The assignment from Berkeley is supported by a mass measurement in a separate step in the same experiment. Furthermore, a comparison of the production cross section and the excitation energy of the compound nucleus derived from the reported beam energy in Ref. [3] shows better compatibility with the $4n$-evaporation channel, leading to ^{245}Md. The $5n$-evaporation channel, leading to ^{244}Md, is less consistent with the cross-section systematics of experimental data and calculations performed using the HIVAP statistical model code for fusion–evaporation reactions [7]. Resolving these inconsistencies is essential both for refining nuclear-structure models near the proton-rich region and for validating statistical-model codes such as HIVAP [8].

The present contribution reports new decay results from an experiment at the Fragment Mass Analyzer (FMA) [9] at Argonne National Laboratory (ANL), performed with identical beam–target combinations as in the previous study at LBNL. The aim is to obtain direct mass identification of nuclei correlated with their α-decay chains, thereby resolving previous ambiguities in mass assignment.

2. Experimental setup and calibration

2.1. The experimental setup

In our study, the reaction ^{209}Bi(^{40}Ar, xn)$^{249-x}$Md was employed, with the ^{40}Ar beam delivered from the linear accelerator of the ATLAS (Argonne Tandem Linac Accelerator System) user facility at ANL at beam energies of $E_{\mathrm{lab}} = 185$–212 MeV. The target consisted of a C–^{209}Bi–C foil sandwich of approximately 40 μg/cm^2–450 μg/cm^2–10 μg/cm^2 in thickness. The targets were fixed to a rotating wheel with 16 segments. An average beam intensity of 205 pnA was used in the experiment.

As illustrated in Fig. 1, the recoils emerging from the target enter the FMA, where they are separated in space based on their mass-over-charge ratio (A/q). The focal plane detectors consisted of a parallel plate avalanche counter (PPAC), followed by a double-sided silicon strip detector (DSSD) where the transmitted ions are implanted. The DSSD was surrounded upstream by single-sided silicon strip detectors (SSSDs) [10]. Five high-purity germanium (HPGe) clover detectors (X-array) were positioned facing the back of the silicon detectors, to record the emitted γ rays [11].

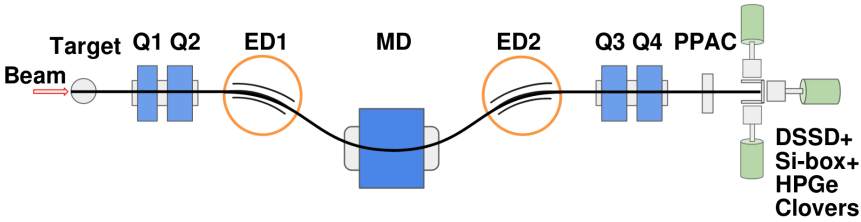

Fig. 1. The schematic representation of the FMA at ANL. Q1, Q2 and Q3, Q4 represent the entry quadrupole doublet and exit quadrupole doublet, respectively. ED1 and ED2 are electric dipoles and MD is a magnetic dipole.

2.2. Calibration of the focal plane detectors of FMA

The reaction ^{174}Yb(^{40}Ar, $[4n, 5n]$)^{209,210}Ra was used to calibrate the focal plane detectors for mass as well as the DSSD for α-decay energies. The reaction has a known cross section of 1.40 ± 0.03 mb for the $4n + 5n$ neutron evaporation channel [12]. The FMA was set to transmit the central charge state 19.5^+ for ^{209}Ra, 17.5^+ for ^{247}Md, and 18.5^+ for ^{245}Md. The FMA allows all particles with A/q within $\pm 4\%$ of the set mass and charge to be transmitted to the focal plane. Position- and time-correlated decay events (α-decay or fission) were recorded in coincidence with the incoming recoil.

The PPAC position distribution for charge states 19^+ and 20^+ for the isotopes ^{208,209,210}Ra was fitted to find the centroids of the different mass distributions, as shown in Fig. 2.

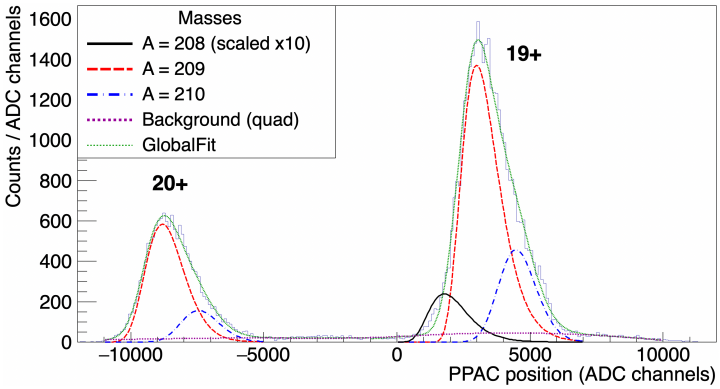

Fig. 2. (Color online) The position of the recoil correlated ^{208,209,210}Ra α-decay events at the PPAC plane. The different-colored curves represent the distribution of masses obtained by fitting each charge state distribution with a double fit function, along with a quadratic background. The red curve (dashed) represents the distribution of ^{209}Ra and the blue curve (dash-dotted) the one for ^{210}Ra. The black curve (solid) represents the distribution of ^{208}Ra, which has been fitted separately and integrated into the same figure.

The A/q values for ^{208,209,210}Ra were plotted as a function of their peak centroids from the fits in Fig. 2. These values were fitted with a linear function, in which the PPAC position (X) is related to the A/q values by the relation

$$X = D\,\frac{\left(\frac{A}{q} - \frac{A_0}{q_0}\right)}{\frac{A_0}{q_0}} + X_0\,. \tag{1}$$

The values of D (slope) and X_0 (intercept) are extracted from the linear regression. The value of the slope is proportional to the dispersion constant of the separator, and the value of the intercept gives the landing position of the nucleus with the central charge state (q_0) of the mass (A_0) to which the setup is tuned. Using the two constants, the central mass and charge values used for the FMA field settings, and Eq. (1), we calculated the expected mass distributions of different charge states produced in the ^{40}Ar + ^{209}Bi reaction at the PPAC position.

In order to validate the setup for mass determination and α-decay energy measurement with an isotope closer to ^{245}Md, mass measurement and decay spectroscopy were performed for ^{247}Md. We used the beam energies $E_{\rm lab}$ = 185 and 187 MeV, and $E_{\rm lab}$ = 210 and 212 MeV for the production of ^{247}Md and ^{245}Md, respectively.

3. Results and discussion

3.1. ^{247}Md

At the beam energies of $E_{\mathrm{lab}} = 185$ and 187 MeV, a total of 13 correlated α-decay events were detected, 11 of which were recorded with full energy deposition in the DSSD. For the first-generation decay, two α-decay energy lines were observed at $E_\alpha = 8.44 \pm 0.03$ MeV and $E_\alpha = 8.70 \pm 0.03$ MeV, with half-lives of $1.5^{+0.5}_{-0.3}$ s and $0.1^{+0.4}_{-0.1}$ s, respectively. The lower α-decay energy is compatible with a ground-state transition, whereas the higher-energy decay corresponds to a transition from its isomeric state as observed in Ref. [13]. In four of these decay chains subsequent α–α correlations were observed and found to be consistent with the ^{243}Es $\rightarrow$ ^{239}Bk α decay with a measured α energy of $E_\alpha = 7.91 \pm 0.03$ MeV and a half-life of $17.7^{+17.0}_{-7.8}$ s. The α-decay energies and the half-lives are consistent with the previous studies of the same isotope at GSI [13]. Also, a single correlated fission event was observed. The quoted α-decay energy uncertainties are derived from the detector energy resolution of 30 keV (FWHM), defining a ± 2.35 σ interval around the measured value for single-event energies.

The position of the recoils correlated with the α-decays at the focal plane of the FMA is shown in Fig. 3. They are compared to the expected positions of masses 246, 247, and 248 for the charge states 17^+ and 18^+. The measured focal plane positions of correlated decays were compared with calibrated A/q values, yielding probabilistic assignments (see Table 1).

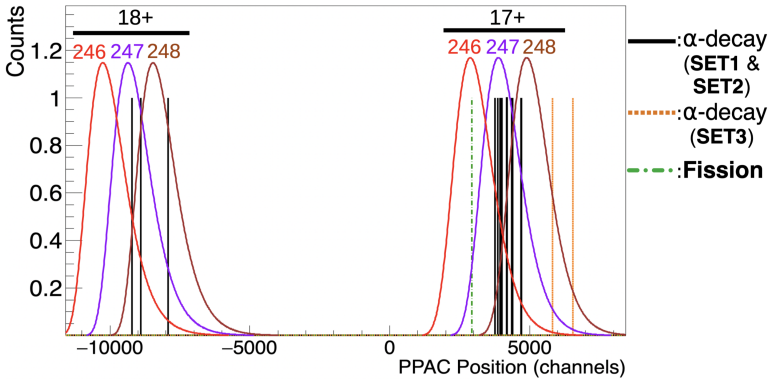

Fig. 3. (Color online) The solid curves represent the expected mass distribution at the focal plane for the two charge states for masses 246, 247 and 248. The black lines (solid) indicate recoils correlated with the α-decays of ^{247}Md, while the orange lines (dotted) denote α-decay events attributed to ^{248}Md. The green line (dash-dotted) corresponds to the fission event.

Table 1. Average mass-assignment probabilities for correlated α and fission events of mendelevium at beam energies of 185 and 187 MeV.

Event type	$A = 246$	$A = 247$	$A = 248$
SET1 ($q = 18^+$)	11%	38%	51%
Fission ($q = 17^+$)	84.3%	15.7%	0%
SET2 ($q = 17^+$)	17%	51%	32%
SET3 ($q = 17^+$)	2.7%	13%	84.3%

As seen in Fig. 2, the mass distributions were not fully resolved but allowed us to make a probabilistic mass-assignment based on the Bayesian formalism [14]. As shown in Table 1, the α-correlated Md recoils of **SET2** can be assigned with $\approx 51\%$ probability to $A = 247$. The correlated recoils to the two α events of **SET3** at the extreme right of the distribution can be assigned with $\approx 84.3\%$ probability to $A = 248$. The α-correlated recoils in the 18^+ charge state (**SET1**), although showing a higher possibility of belonging to $A = 248$, exhibit α-decay energies and decay times consistent with known ^{247}Md decays from previous experiments [13]. The reason for the broadening of the recoil distribution for the higher-charge state is still unknown and will be investigated.

3.2. ^{245}*Md*

Following the same methodology as for ^{247}Md, beam energies of $E_{\text{lab}} =$ 210 and 212 MeV were employed to study ^{245}Md. The beam energy $E_{\text{lab}} =$ 210 MeV is the same as that deduced from the experimental information reported in a previous study by Pore *et al.* [3], taking into account the energy loss in the 2.1 μm thick titanium backing. At $E_{\text{lab}} = 212$ MeV, one correlated α-decay was observed, consistent with the decay energy and half-life reported in both Md experiments at GSI [4] and Berkeley [3]. The event has an α-decay energy of 8.69 ± 0.03 MeV with a half-life of $0.17^{+0.62}_{-0.15}$ s. This event was also found to be correlated with a second α-decay of energy 8.12 ± 0.03 MeV and half-life of $0.25^{+0.92}_{-0.22}$ s, which is consistent with the α-decay energy and decay half-life of ^{241}Es [2]. In addition to the single α-decay, three fission events were also observed, with decay times on the order of tens of μs.

The same procedure as applied for ^{247}Md (see Section 3.1) was followed for the mass identification of the α-correlated recoil of ^{245}Md. It was observed that the α-correlated event is more probable to be ^{245}Md.

3.3. Cross-section calculation

From these results, the following production cross sections were calculated for ^{245,247}Md at different beam energies, taking into account the beam dose, target thickness, and separator transmission

$$\sigma\left(^{247}\mathrm{Md}, E_{\mathrm{beam}} = 187\ \mathrm{MeV}\right) = 6.9^{+4.6}_{-2.9}\ \mathrm{nb}\,,$$
$$\sigma\left(^{247}\mathrm{Md}, E_{\mathrm{beam}} = 185\ \mathrm{MeV}\right) = 2.6^{+1.3}_{-1.9}\ \mathrm{nb}\,,$$
$$\sigma\left(^{245}\mathrm{Md}, E_{\mathrm{beam}} = 212\ \mathrm{MeV}\right) = 101^{+320}_{-90}\ \mathrm{pb}\,.$$

The cross section for ^{245}Md measured in this work confirms the compatibility with the $4n$-evaporation channel at a beam energy 2 MeV higher than that reported in Ref. [3] (see Fig. 4).

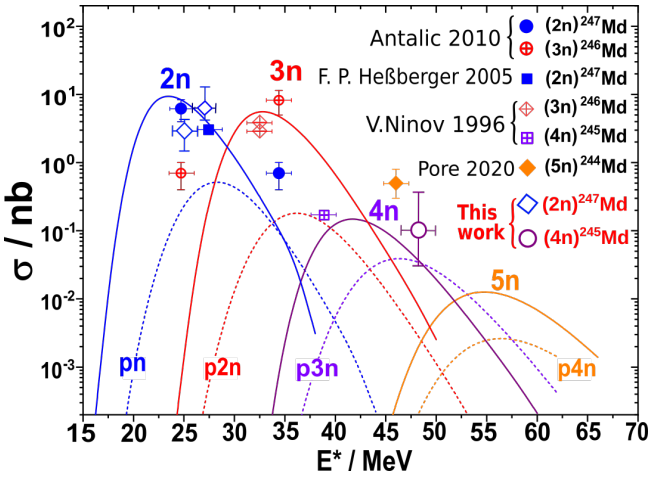

Fig. 4. Plot of the production cross section as a function of excitation energy for the reaction ^{40}Ar + ^{209}Bi, calculated using the HIVAP statistical model (adapted from Ref. [7]). The solid line represents the neutron (n) evaporation channels, and the dashed line represents the proton–neutron (p–xn) evaporation channels. The results from different experiments, along with the results from the current analysis, are shown in the plot.

4. Conclusions

At the FMA, the ^{209}Bi(^{40}Ar,xn)$^{249-x}$Md reaction was used to identify thirteen recoil-α-decay chains of ^{247}Md and one recoil-α–α decay chain of ^{245}Md. A provisional mass assignment of the recoils was performed.

Mass-assignment probabilities derived from calibrated A/q spectra do not support the mass-assignment reported by Pore *et al.* [3]. The new FMA data clarify several unresolved questions regarding light Md isotopes: The

α-decay energies observed for the correlated decay chain of ^{245}Md align with previously reported values from the GSI and Berkeley studies. Furthermore, the A/q analysis indicates that the α-decay originates with the highest probability from Md of mass $A = 245$. The deduced cross sections from our measurements for ^{247}Md and ^{245}Md are consistent with HIVAP calculations.

This work was partly funded by the Region Normandie under the grant RIN Doctorants. This experiment was supported by the U.S. Department of Energy, Office of Nuclear Physics, under award No. DE-AC02-06CH11357. This study used resources of ANL's ATLAS facility, which is a DOE Office of Science User Facility. We also acknowledge the support of the France North-America Network on the Physics of Exotic Nuclei (FANPEN), the Slovak Research and Development Agency (contract No. APVV-22-0282) and Scientific Grant Agency VEGA (contract No. 1/0019/25). S. Kumar further acknowledges the COPIGAL Collaboration for financial support for his conference participation.

REFERENCES

[1] R.R. Chasman, I. Ahmad, A.M. Friedman, J.R. Erskine, *Rev. Mod. Phys.* **49**, 833 (1977).
[2] V. Ninov *et al.*, *Z. Phys. A* **356**, 11 (1996).
[3] J.L. Pore *et al.*, *Phys. Rev. Lett.* **124**, 252502 (2020).
[4] J. Khuyagbaatar *et al.*, *Phys. Rev. Lett.* **125**, 142504 (2020).
[5] A. Semchenkov *et al.*, *Nucl. Instrum. Methods Phys. Res. B* **266**, 4153 (2008).
[6] V. Ninov, K.E. Gregorich, C.A. McGrath, *AIP Conf. Proc.* **455**, 704 (1998).
[7] F.P. Heßberger *et al.*, *Phys. Rev. Lett.* **126**, 182501 (2021).
[8] W. Reisdorf, M. Schädel, *Z. Phys. A* **343**, 47 (1992).
[9] C.N. Davids *et al.*, *Nucl. Instrum. Methods Phys. Res. B* **70**, 358 (1992).
[10] https://www.phy.anl.gov/fma/dssd.html
[11] A.J. Mitchell *et al.*, *Nucl. Instrum. Methods Phys. Res. A* **763**, 232 (2014).
[12] D. Vermeulen *et al.*, *Z. Phys. A* **318**, 157 (1984).
[13] F.P. Heßberger *et al.*, *Eur. Phys. J. A* **58**, 11 (2022).
[14] A. Mikhalychev *et al.*, *Ultramicroscopy* **215**, 113014 (2020).